**Cell Systems, Volume *6***

## Supplemental Information

# Reserve Flux Capacity in the Pentose Phosphate Pathway Enables *Escherichia coli*'s Rapid Response to Oxidative Stress

**Dimitris Christodoulou, Hannes Link, Tobias Fuhrer, Karl Kochanowski, Luca Gerosa, and Uwe Sauer**

# Supplemental Information

## Reserve flux capacity in the pentose phosphate pathway enables *Escherichia coli*'s rapid response to oxidative stress

Dimitris Christodoulou, Hannes Link, Tobias Fuhrer, Karl Kochanowski, Luca Gerosa, Uwe Sauer

## Supplementary Figures

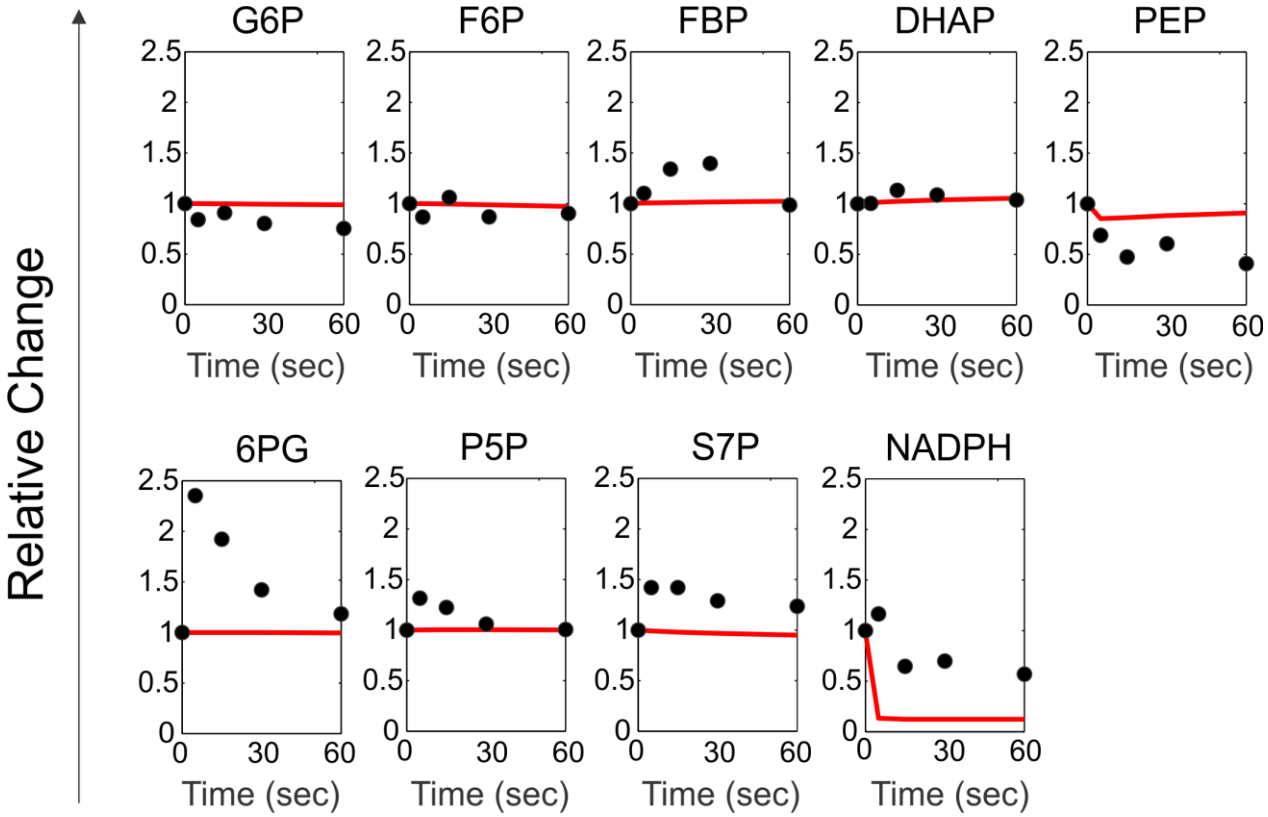


**Figure S1. Related to Figure 5:** Base model (model amended with the ROS inhibition of GAPDH) simulation results (red solid line) against the experimental data (black dots). Y axis represents the relative change of a particular metabolite, compared to the untreated condition (time point 0).

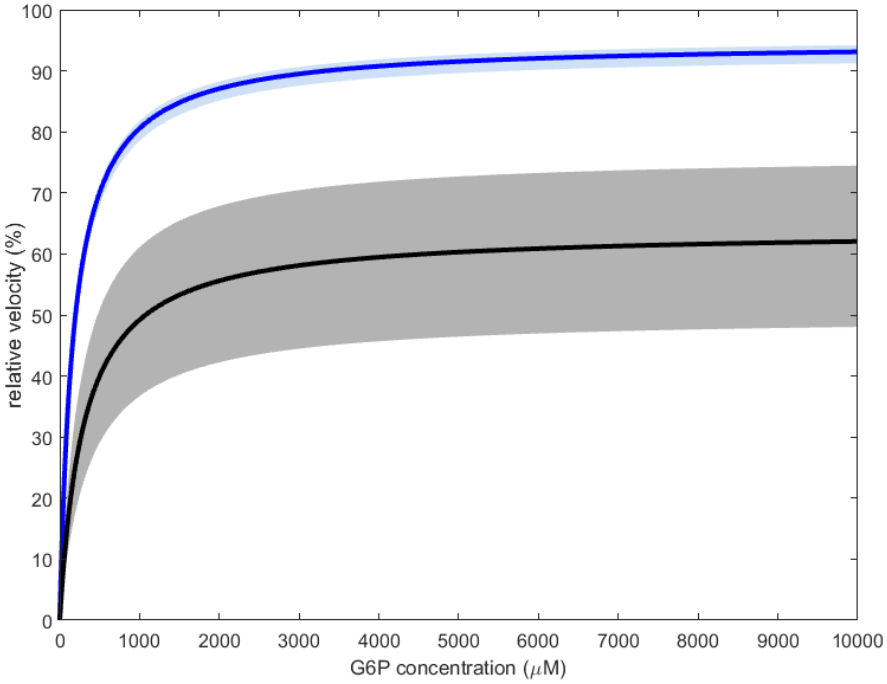


**Figure S2. Related to STAR Methods:** Simulated reaction velocities for glucose-6-phosphate dehydrogenase using rate laws without NADPH inhibition (blue line, Supplementary Methods Equation 1) and with NADPH inhibition (black line, Supplementary Methods Equation 2). Experimentally determined kinetic parameters were used (mean values from Table S1) and the pool of NADPH and $NADP^+$ was assumed to be approximately 500µM, well above measured dissociation, inhibition constants and $K_M$. The shaded areas are created by testing different NADP/NADPH ratios. Only the forward reaction with NADPH inhibition was simulated since the 6P-gluconolactone produced reacts rapidly further to 6P-gluconate and in addition is very instable[1]. G6P concentration during growth on glucose in wild type *E. coli* is in the range of 1-2 mM, with mutant strain Δpgi having approximately 10 times higher concentrations[2].

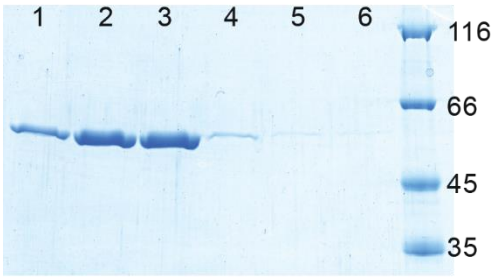


**Figure S3. Related to STAR Methods:** SDS-PAGE of overexpressed and His-Tag purified glucose-6P dehydrogenase (~56.8 kD including His-Tag). The pure enzyme was eluted with different imidazole concentrations (lanes 1 to 6: 100-200, 200, 200-300, 300, and twice 500 mM imidazole). Fractions in lane 2 and 3 were pooled and used for further analysis.

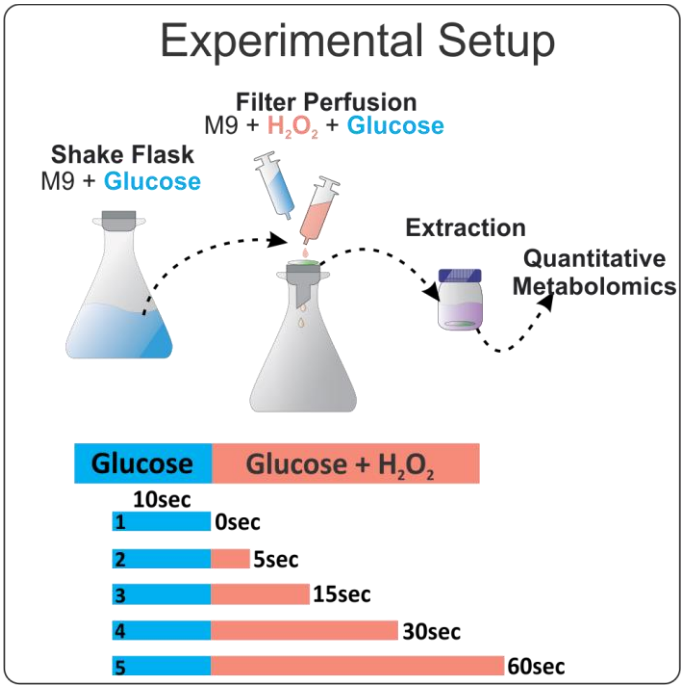


**Figure S4. Related to STAR Methods:** Experimental setup for fast carbon-source switching. Culture broth from a shake flask is transferred onto a nitrocellulose filter mounted on a vacuum device. Subsequently cells are continuously perfused with medium containing glucose and are then switched to a freshly prepared medium containing glucose and $H_2O_2$. Upon filtration the filter is extracted in cold acetonitrile/methanol/water mix and cell extracts are analyzed by ultrahigh performance liquid chromatography– tandem mass spectrometry. Lower panel, perfusion profiles of samples before extraction. Cyan bars, perfusion with glucose medium; orange bars, with glucose and $H_2O_2$ medium.

# Supplementary Tables

**Table S1. Related to Figure 5:** Experimentally determined kinetic parameters of **G6P dehydrogenase** and intracellular metabolite concentrations

| | This study [μM] | Olavarria et al* [μM] |
|---|---|---|
| ***Kinetic Parameters[a]:*** | | |
| ***Substrate $K_M$:*** | | |
| $NADP^+$ | 23 | 7.5 ± 0.8 |
| glucose-6-phosphate | 136 | 174 ± 11 |
| ***$NADP^+$ dissociation $K_i$:*** | | |
| $NADP^+$ | 90 | 19 ± 4 |
| ***NADPH inhibition $K_i$:*** | | |
| $K_{ic,NADP+}$ | 35 | 14 ± 2 |
| $K_{ic,glucose-6-phosphate}$ | 100 | 101 ± 9 |
| ***Relative reaction rates[b]*** | | |
| 2 mM Fructose- 1,6-bisphosphate (FBP) | 98 | - |

[a] Own values were obtained from primary and secondary Lineweaver-Burk plots and were confirmed by non-linear regression fits with the corresponding rate laws.

[b] Normalized to reaction rate in absence of inhibitor, using 25 μM $NADP^+$ and 125 μM as substrate, standard deviations were below 5% from triplicate experiments.

* Olavarría, K., Valdés, D. & Cabrera, R. The cofactor preference of glucose-6-phosphate dehydrogenase from Escherichia coli--modeling the physiological production of reduced cofactors. *FEBS J.* **279,** 2296–309 (2012).

**Table S2. Related to Figure 3:** Kinetic parameters of reactions in the glycolysis – PP pathway model. $V_{max}$ of irreversible reactions are estimable parameters and no value is given.

| Reaction | Parameter | Value Range |
|---|---|---|
| **Irreversible Reactions** | | |
| PFK | $V_{max,PFK}$ | - |
| | $K_{PFK,F6P}$ | $(0.1\text{-}10) \cdot 0.16\text{mM}$[1] |
| FBPase | $V_{max,FBPase}$ | - |
| | $K_{FBPase,FBP}$ | $(0.1\text{-}10) \cdot 0.015\text{mM}$[2] |
| G6PDH | $V_{max,\ G6PDH}$ | - |
| | $K_{G6PDH,G6P}$ | $(0.1\text{-}10) \cdot 0.2\text{mM}$[3] |
| GND | $V_{max,GND}$ | - |
| | $K_{GND,6PG}$ | $(0.1\text{-}10) \cdot 0.1\text{mM}$[4] |
| PYK | $V_{max,PYK}$ | - |
| | $K_{PYK,PEP}$ | $(0.1\text{-}10) \cdot 0.31\text{mM}$[5] |
| PPS | $V_{max,PPS}$ | - |
| | $K_{PPS,PYR}$ | $(0.1\text{-}10) \cdot 0.083\text{mM}$[6] |
| PDH | $V_{max,PDH}$ | - |
| | $K_{PDH,PYR}$ | $(0.1\text{-}10) \cdot 0.515\text{mM}$[7] |
| PPC | $V_{max,PPC}$ | - |
| | $K_{PPC,PEP}$ | $(0.1\text{-}10) \cdot 0.19\text{mM}$[8] |


1. Zheng, R. L. & Kemp, R. G. The mechanism of ATP inhibition of wild type and mutant phosphofructo-1-kinase from Escherichia coli. *J. Biol. Chem.* **267,** 23640–5 (1992).
2. Kelley-Loughnane, N. *et al.* Purification, kinetic studies, and homology model of Escherichia coli fructose-1,6-bisphosphatase. *Biochim. Biophys. Acta - Protein Struct. Mol. Enzymol.* **1594,** 6–16 (2002).
3. Westwood, A. W. & Doelle, H. W. Glucose 6-phosphate and 6-phosphogluconate dehydrogenases and their control mechanisms in Escherichia coli K-12. *Microbios* **9,** 143–65 (1974).
4. de Silva, A. O. & Fraenkel, D. G. The 6-phosphogluconate dehydrogenase reaction in Escherichia coli. *J. Biol. Chem.* **254,** 10237–42 (1979).
5. Boiteux, A., Markus, M., Plesser, T., Hess, B. & Malcovati, M. Analysis of progress curves. Interaction of pyruvate kinase from Escherichia coli with fructose 1,6-bisphosphate and calcium ions. *Biochem. J.* **211,** 631–40 (1983).
6. Berman, K. M. & Cohn, M. Phosphoenolpyruvate synthetase of Escherichia coli. Purification, some properties, and the role of divalent metal ions. *J. Biol. Chem.* **245,** 5309–18 (1970).
7. Nemeria, N. *et al.* Inhibition of the Escherichia coli Pyruvate Dehydrogenase Complex E1 Subunit and Its Tyrosine 177 Variants by Thiamin 2-Thiazolone and Thiamin 2-Thiothiazolone Diphosphates: EVIDENCE FOR REVERSIBLE TIGHT-BINDING INHIBITION. *J. Biol. Chem.* **276,** 45969–45978 (2001).
8. Kai, Y. *et al.* Three-dimensional structure of phosphoenolpyruvate carboxylase: a proposed mechanism for allosteric inhibition. *Proc. Natl. Acad. Sci. U. S. A.* **96,** 823–8 (1999).

**Table S3. Related to Table 1:** Rank of the interactions, as inferred from our combined computational-experimental approach. Pairwise average rank ($5^{th}$ column) was calculated as the average of the different ranks each interaction achieved in individual metrics, namely frequency and score, stemming from the results of approximately 24 million pairwise simulations. Enzymes affected by metabolites (activated or inhibited) are shown in columns 2, 3 and 4 of the table, respectively.

**Table S4. Related to Table 1:** Rank of all 162 interactions that were tested in models with pairwise allosteric interactions. Both frequency and score metrics are displayed. Ranking is based on how often the interaction appears in models with ΔAIC>0 (frequency).

**Table S5. Related to Table 1:** Rank of all 162 interactions displaying the AIC of models with single interactions relative to the base model. Ranking is based on the best ΔAIC that was achieved with a model including only this interaction.

**Table S6. Related to Figure 1, Figure 2 and STAR Methods:** Metabolite data of the $H_2O_2$ perturbation. The standard deviation (s.d.) results from three independent experiments. Time (in seconds) demonstrates the time of exposure to $H_2O_2$, after 10 seconds washing with glucose minimal medium (see STAR Methods)